JOURNAL OF COMPUTATIONAL PHYSICS 32, 254–262 (1979)

Note

The Method of Differential Areas for Computing Crystal Symmetry Independent Density of States Spectra*

The differential area method for calculating joint density of states spectra given any electron or phonon dispersion relation is explained. Examples of this procedure are to nearest and next nearest neighbor phonon spectra in the harmonic approximation and to an electron network model of diatomic crystals. The advantages of this technique are that it is completely crystal symmetry independent, does not require any root searching of frequency or energy ranges, and can be utilized irrespective of the nature of the force model employed. Excluding initialization, the computer code in the MATHSY array language available at the Lawrence Livermore Laboratory is only 15 lines long.

In this note we shall briefly describe an accurate and simply applied algorithm for computing the joint density of states energy or frequency spectrum arising in solid state physics. The method is totally crystal symmetry independent, does not require any root searching or gradient computations, may be preset to any desired energy or frequency range, and can be utilized irrespective of the nature of force model employed.

Related to a geometrical approach developed by Budgor and Poston [1, 2] and intuited by Leighton [3] and Faulkner *et al.* [4] this technique has the attractive feature of being able to visually examine the constant frequency or energy contours in the Brillouin zone from which the spectra are derived. Thus, the occurrence and location of spectral singularities can be predicted and verified by simultaneous comparison of contours with spectra.

Methodologically, all we require are the elements of a dynamical frequency or connectivity energy matrix $M(\mathbf{q})$, whose determinant equated to zero yields a dispersion relation governing how the frequency or energy variables (denoted by x) are distributed in the Brillouin zone. For convenience we rescale the reciprocal lattice vector $\mathbf{q} = (q_1, q_2, q_3)$ so that the volume of the Brillouin zone is unity. We then subdivide the Brillouin zone into m equi-distant planes—i.e., $q_1 - q_2$ planes, $q_3 =$ constant—each containing its respective energy or frequency contours produced by the dispersion relation. The *differential area method* partitions a given preset x span, $x_{\min} \leqslant x \leqslant x_{\max}$, into r intervals and performs the operation

$$P(x_l, x_{l+1}) = \det \mid M(\mathbf{q})|_{x_l} \cdot \det \mid M(\mathbf{q})|_{x_{l+1}} \qquad l = 1,\ldots, r+1 \tag{1}$$

* Work performed under the auspices of the U. S. Department of Energy under contract No. W-7405-Eng-48.

0021-9991/79/080254–09$02.00/0

for each endpoint $x = x_l$ value on each plane. The planar density of states is by definition the differential area between curves of constant x_l and x_{l+1}. Numerically this is equivalent to the integrated Brillouin zone area of sequential zero crossings of det $|M(\mathbf{q})|$ between these adjacent x values; geometrically it is proportional to the movement of those curves. The total number of zero crossings is sensed by $P(x_l, x_{l+1})$ and the spectrum value $D(x_{l+1})$ is approximately equal to the number of points for which P is negative (the distance between the zeros of the two factors in Eq. (1)), with $D(x)$ the histogram of all $D(x_l)$. This procedure for calculating $D(x)$ can be shown to be numerically identical to the δ-function representation for the density of states [6]. Figure 1 illustrates how $D(x_l)$ is computed. As this procedure is to be carried out for each plane, the composite $D(x)$ is the cumulative sum of all planar $D(x)$ spectra normalized to the Brillouin zone volume. This normalization is obtained upon multiplying each $D(x_l)$ by the factor $[(n_1)(n_2)(m)(x_{l+1} - x_l)]^{-1}$, n_1 and n_2 being,

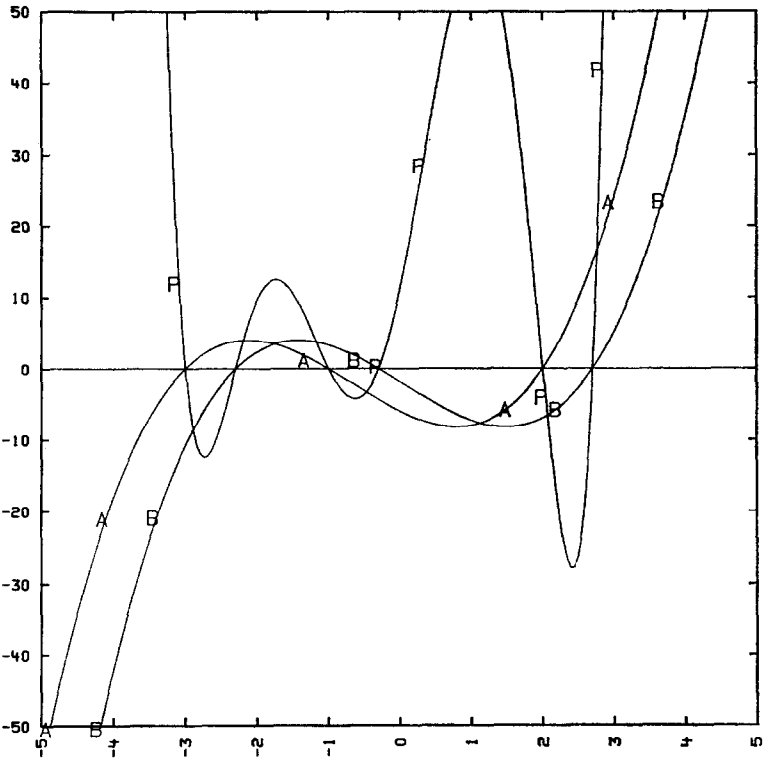

FIG. 1. Illustration of how $D(x_l)$ is computed. Each q_3 plane of the Brillouin zone is partitioned into a number of $q_1 - q_2$ — mesh size dependent boxes. Schematically, if curves A and B represent the factors of the product curve P (comprised on n grid points) for some $l = t$, then $D(x_l)$ is related to the distance between the sequential zero crossings of A and B within each $q_1 - q_2$ box. In this figure this occurs where P is negative and approximately equals the number of points, $s \leqslant n$ say, at which it is negative. This approximation becomes more exact upon refinement of the $q_1 - q_2$ mesh size.

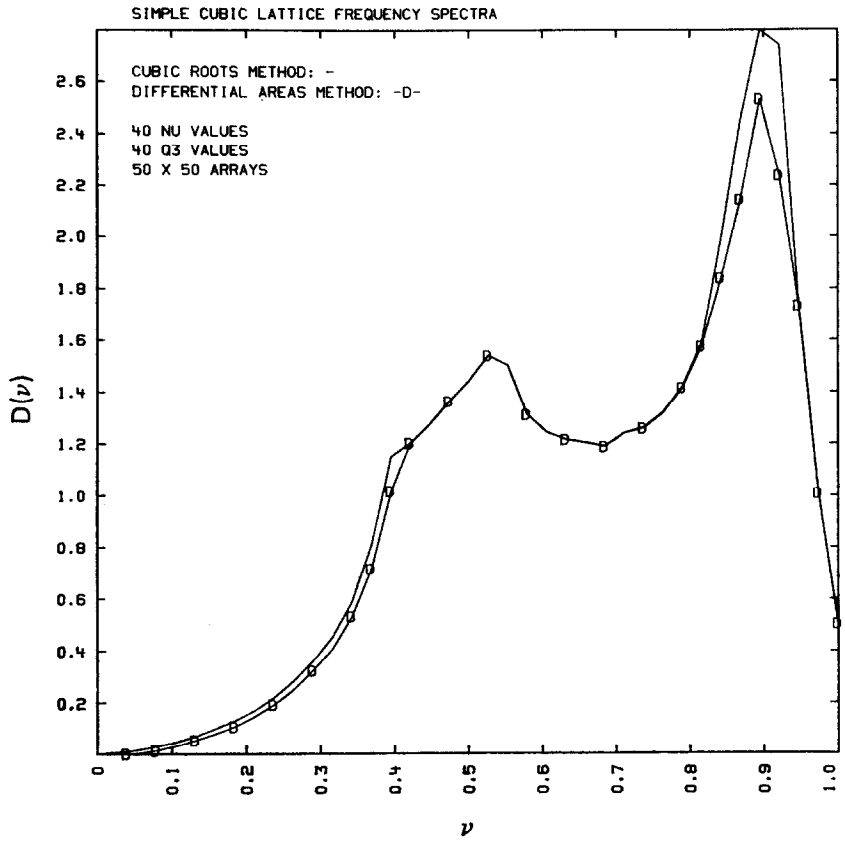

FIG. 2. Comparison of $D(\nu)$ between the root surface (solid lined) and differential area (D-lined) methods for a simple cubic lattice with nearest and next-nearest neighbor force constants set at $\alpha = 0.175$ and $\gamma = 0.01875$. $D(\nu)$ is generated with 40ν values, $40q_3$ values, and a 50×50 $q_1 - q_2$ array. *CPU* times are 0.5 min. for the root surface method and 1.3 min. for the differential area method.

respectively, the number of grid points into which q_1 and q_2 are subdivided. When $M(\mathbf{q})$ is made up of a number of branches, this resultant $D(x)$ is the combined or joint contribution from all branches.

Figures 2–4 exhibit representative $D(x)$ spectra for both a lattice vibration and a one-electron energy case. Example plane by plane contour developments from which these $D(x)$ are derived are shown in Fig. 5. In the former example the phonon $D(\nu)$ correspond to the cubic lattices with nearest and next-nearest neighbor spring constants in the harmonic approximation. The form of these spectra are already known [3, 5] and a much more extensive accounting of the details of the computation will be presented elsewhere [6, 7]. The D-lined spectra in Figs. 2 and 3 were produced by the differential area method. They are compared with the solid lined spectra (root surface method) produced by analytically obtaining the individual branch spectra from the

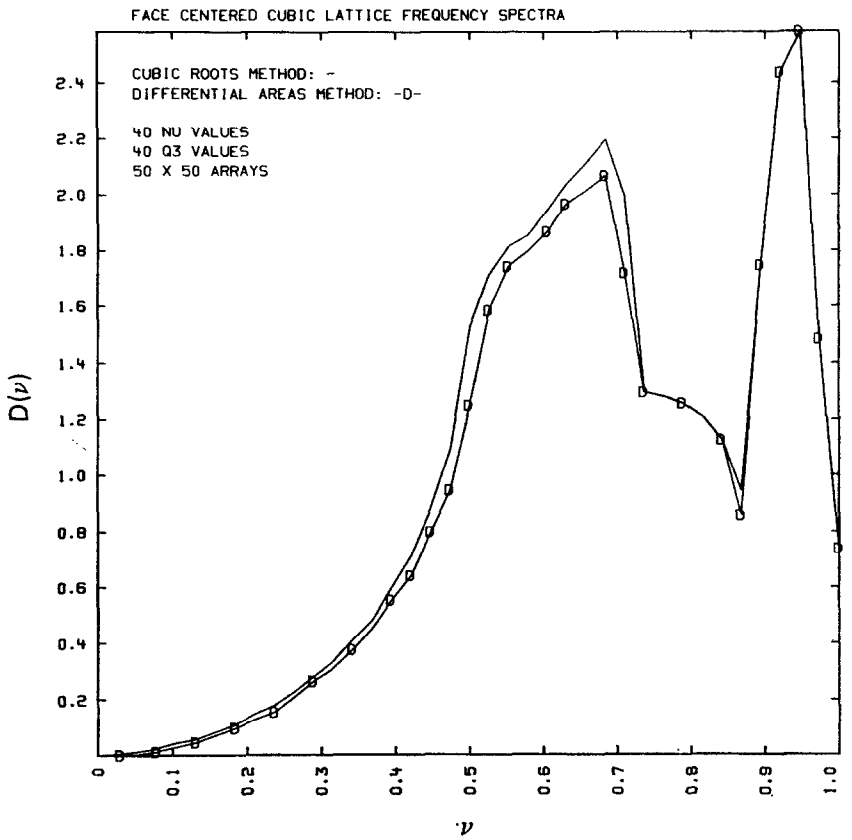

FIG. 3. Comparison of $D(\nu)$ between the root surface (solid lined) and differential area (D-lined) methods for a face centered cubic lattice with $\gamma/\alpha = 0$. Same initial mesh size data and *CPU* times as for Fig. 2.

dispersion relations and summing their contributions [6, 7]. Although both curves have exactly the same shape, the values of $D(\nu)$ found by the differential area method are slightly lower than those found by the root surface method. This seems to result from the fact that the differential area method suffers from degeneracy error whenever points or lines from the same constant ν-valued branches are coincident. As is apparent, however, with a fine enough ν and Brillouin zone $\mathbf{q}$ mesh size, this error is not very great. *CPU* times for the differential area method are in general longer than those for the root surface method since complete $q_1 - q_2$ surfaces are generated for each ν_l value.

Our second example of diatomic cubic lattices is derived from a one electron network bonding model of molecules and crystals in which the electrons are restricted to lie only along the bonds of the material [8, 9]. If we further simplify this characterization and make these "bonds" one dimensional, then the electronic properties of our network model of "lines" and "point atoms" are topological in origin and are

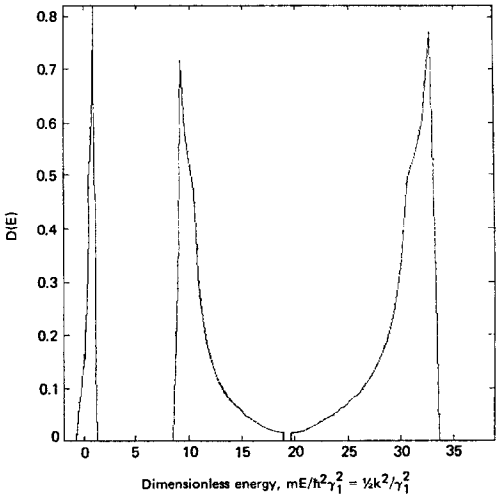

FIG. 4. $D(E)$ for a diatomic face centered cubic lattice with dispersion relation given by (6c). The well-depth parameters γ_1 and γ_2 are, respectively, $\gamma_1 = 1$ and $\gamma_2 = 0.5\gamma_1$; the bondlength l is $l = 1$. $D(E)$ was generated with $15E$ values in the first band, $100E$ values in the second band, $40q_3$ values, and a $70 \times 70q_1 - q_2$ array. The *CPU* time was 4.8 min. Note the occurrence of band gaps between energies $1.1 < E < 8.3$ and $18.3 < E < 20$.

solely determined by the degree of "bonding" [10, 11]. We simulate bonding by choosing for our one electron atomic potential the bound "soliton"

$$V(x) = -\frac{\hbar^2\gamma^2}{2m} s(s+1) \operatorname{sech}^2 \gamma x \tag{2}$$

which in its limiting forms embodies both the extremely localized Heitler–London and delocalized Bloch models. Thus, as the well-depth parameter $\gamma \to 0$ $V(x)$ reduces to the Sommerfeld free electron model and as $\gamma \to \infty$ $V(x)$ approaches a tight binding potential. γ is, therefore, related to an effective mass and its variation permits description leading from covalency to ionicity. Energy line and band spectra are derivable in a manner analogous to *LCAO* and tight binding computations which yields a form factor equation relating the amplitude of the wave function $\psi(j)$ of one atom at site j to its n_j bonded atoms at sites j_ρ ,

$$n_j F(k, \gamma)\, \psi(j) = \sum_{j_\rho} \psi(j_\rho) \tag{3}$$

All the characteristics of the potential $V(x)$ are embedded in $F(k, \gamma)$, which for a diatomic lattice has the form

$$F(k_1, \gamma_1, \gamma_2) = \frac{\alpha_1(F_1K_2 - H_1G_2) + \alpha_2(F_2K_1 - H_2G_1)}{2\alpha_1\alpha_2} \tag{4}$$

where

$$\alpha_1 = 1 + (\gamma_1/k)^2,\ \alpha_2 = 1 + (\gamma_2/k)^2$$

and

$$\begin{aligned} F_i &= \cos kl - (\gamma_i/k) \sin kl \tanh \gamma_i l \\ G_i &= \sin kl + (\gamma_i/k) \cos kl \tanh \gamma_i l \\ H_i &= G_i + (\gamma_i/k)^2 \sin kl \operatorname{sech}^2 \gamma_i l \\ K_i &= F_i + (\gamma_i/k)^2 \cos kl \operatorname{sech}^2 \gamma_i l \end{aligned} \tag{5}$$

In deriving (4) we have assumed a unit cell length of $2l$. k is a dimensionless energy parameter, $k^2 = 2mE/\hbar^2$.

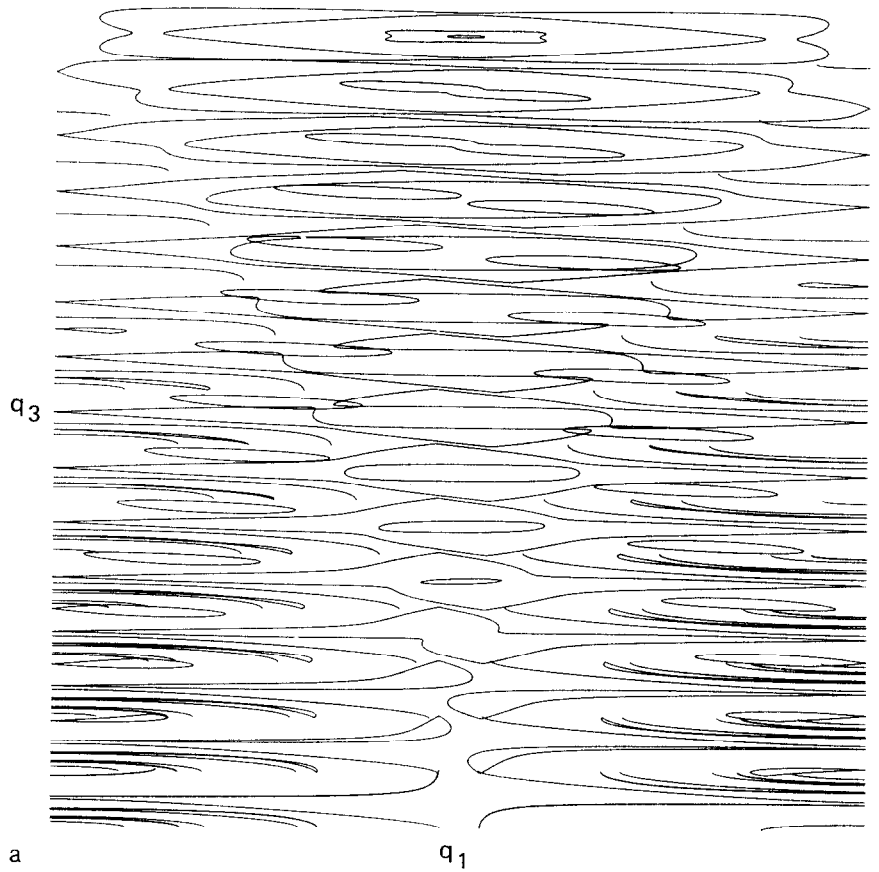

FIG. 5. Superposition of sets of $q_1 - q_2$ planar slices for various values of q_3 = constant. The Brillouin zone is being viewed slightly off the q_2-axis. This permits $3 - D$ visualization of how the contours develop in $\mathbf{q}$ space. (a) Frequency contours for body centered cubic lattice; $15q_3$ slices with $\mathbf{q}$ lying in $[0, \pi] \times [0, \pi] \times [0, \pi/2]$.

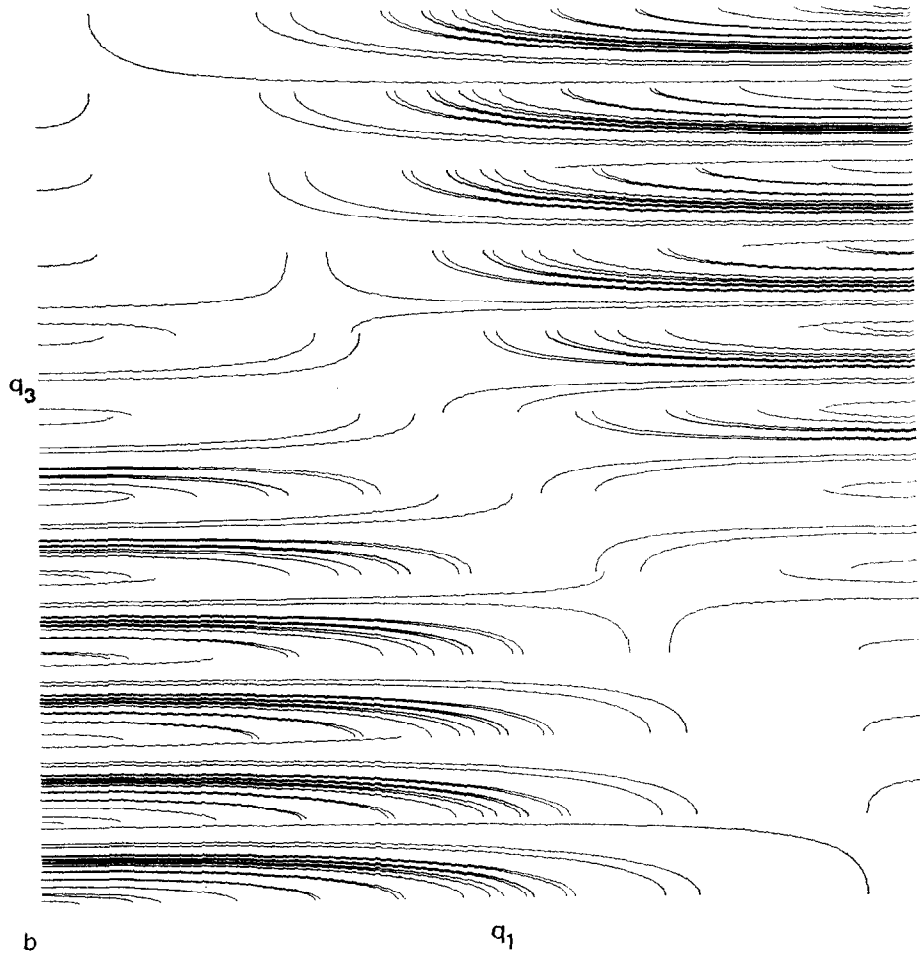

FIG. 5. (b) Energy contours for diatomic face centered cubic lattice; $10q_3$ slices with $\mathbf{q}$ lying in $[0, \pi] \times [0, \pi] \times [0, \pi]$.

Inserting (4) into the form factor eq. (3) with the appropriate crystal symmetry yields the electron connectivity matrix $M(\mathbf{q})$. Band energies are obtained from the dispersion relation $\det | M(\mathbf{q}) | = 0$; these for nearest neighbor simple cubic, body centered cubic, and face centered cubic are

$$s.c. \quad 3F = \cos q_1 + \cos q_2 + \cos q_3 \tag{6a}$$

$$b.c. \quad 3F = \cos q_1 \cos q_2 \cos q_3 \tag{6b}$$

$$f.c. \quad 3F = \cos q_1 \cos q_2 + \cos q_1 \cos q_3 + \cos q_2 \cos q_3 \tag{6c}$$

Although $M(\mathbf{q})$ is a symmetrical matrix the manipulations leading to (5) do not involve a linear eigenvalue problem, as do the harmonic dynamical matrices and the

tight-binding electron connectivity matrices, since $E(\mathbf{q})$ is related nonlinearly to the dispersion relations. Thus, in evaluating $D(E)$ root-searching and moments methods are either impossible or very difficult to implement. This however, does not produce any problems for our method since only endpoint values of any E span, such as the E value at the bottom and top of any band, are required as input parameters. These values can be obtained either numerically (ascertaining those values of E for which $F = \pm 1$) or their approximate locations can be determined by plotting F as a function of E.

In closing we would like to mention that both the vibrational and electronic examples discussed were chosen since their dispersion relations were mathematically sufficiently complex to produce nontrivial $D(x)$ spectra. It should be clear, however, that no matter how the x limits are found, for example the E limits from an *APW* or a muffin-tin calculation, or even from raw empirical data, one could easily employ the differential area method to yield an accurate $D(x)$. Secondly, since exactly the same program operations, i.e., eq. (1) and subsequently counting the number of points for which P is negative, are performed regardless of the crystal symmetry, this technique is completely crystal symmetry independent.

One final point on *CPU* times; for this particular example the differential area *CPU* time is slightly greater than the root surface *CPU* time since the three branches of the cubic lattice in the Brillouin zone are expressed analytically. For more complicated atomic or molecular crystals root surface or other root searching routines such as Gilat–Raubenheimer [12] *CPU* times dramatically increase while the *CPU* time for the differential area method will stay basically the same. This is due to the fact that the number of operations determining the number of negative points of (1) remain the same regardless of the size of the determinant. Thus, spectra derived from high order secular (or non-secular) determinants can be found as easily as the spectra for the cubic lattice problems studied in this note. The computer code used to produce both contours and spectra, excluding initialization, was written in the MATHSY array language which is available at the Lawrence Livermore Laboratory, and is 15 lines long. [6, 7, 13] All computations were performed on a *CDC* 7600.

ACKNOWLEDGMENT

I sincerely thank Giles Peterson for many interesting conversations and for helping in the computations.

REFERENCES

1. A. B. BUDGOR, Ph. D. thesis, University of Rochester, 1974.
2. T. POSTON AND A. B. BUDGOR, *J. Computational Physics* **19** (1975), 1.
3. R. B. LEIGHTON, *Rev. Modern Phys.* **20** (1948), 165.
4. J. S. FAULKNER, H. L. DAVIS, AND H. W. JOY, *Phys. Rev.* **161** (1967), 656.
5. E. W. MONTROLL, *J. Chem. Phys.* **11** (1943), 481; E. W. MONTROLL AND D. C. PEASLEE, *J. Chem. Phys.* **12** (1944), 98.
6. A. B. BUDGOR AND G. PETERSON, Lawrence Livermore Laboratory, Report UCRL-80744, 1978.

7. G. PETERSON AND A. B. BUDGOR, Lawrence Livermore Laboratory, Report UCRL-81088, 1978.
8. J. R. PLATT, "Free Electron Theory of Conjugated Molecules," Wiley, New York, 1964.
9. E. W. MONTROLL, *J. Math. Phys.* **11** (1970), 635.
10. A. B. BUDGOR, *J. Math. Phys.* **17** (1976), 1538.
11. A. B. BUDGOR, *in* "Tunneling in Biological Systems" (B. Chance *et al.*, Eds.), p. 77, Academic Press, New York, 1979.
12. G. GILAT AND L. J. RAUBENHEIMER, *Phys. Rev.* **144** (1966), 390.
13. G. PETERSON, "MATHSY Report." Copies may be obtained by contacting the author at Lawrence Livermore Lab., P. O. Box 808, Livermore, Calif. 94550.

RECEIVED: June 6, 1978; REVISED: September 29, 1978

AARON B. BUDGOR
Lawrence Livermore Laboratory
University of California
Livermore, California 94550